

Article

Angiogenesis Driven by the CEBPD–hsa-miR-429–VEGFA Signaling Axis Promotes Urothelial Carcinoma Progression

Ti-Chun Chan ^{1,2}, Chung-Hsi Hsing ¹, Yow-Ling Shiue ³ , Steven K. Huang ^{1,4}, Kun-Lin Hsieh ¹, Yu-Hsuan Kuo ^{1,5}  and Chien-Feng Li ^{1,2,3,*} 

¹ Chi Mei Medical Center, Tainan 71004, Taiwan; 090807@nhri.edu.tw (T.-C.C.); hsing@mail.chimei.org.tw (C.-H.H.); cmh7530@mail.chimei.org.tw (S.K.H.); 990707@mail.chimei.org.tw (K.-L.H.); a10901@mail.chimei.org.tw (Y.-H.K.)

² National Health Research Institutes, National Institute of Cancer Research, Tainan 70456, Taiwan

³ Institute of Precision Medicine, National Sun Yat-sen University, Kaohsiung 804201, Taiwan; shirley@imst.nsysu.edu.tw

⁴ Department of Biotechnology, Chia Nan University of Pharmacy and Science, Tainan 71710, Taiwan

⁵ College of Pharmacy and Science, Chia Nan University, Tainan 71710, Taiwan

* Correspondence: angelo.p@yahoo.com.tw; Tel.: +886-6-2812811 (ext. 53680); Fax: +886-6-2511235

Abstract: Background and Purpose: This research aimed to excavate the alternative mechanism of CEBPD on tumor growth and explore the biological significance of the CEBPD/hsa-miR-429/VEGFA axis on angiogenesis in urothelial carcinoma (UC). Methods: Quantitative RT-PCR, immunoblotting assay and tube formation examined the effect of hsa-miR-429 mimic or/and inhibitor on VEGFA expression and angiogenesis in CEBPD-overexpressing UC-derived cells. The association between CEBPD, hsa-miR-429, VEGFA and microvascular density (MVD) and clinical outcome were evaluated in 296 patients with UBUC and 340 patients with UTUC, respectively. Results: The increase in the transcript and protein of VEGFA as well as HUVECs tube formation was diminished upon the treatment of hsa-miR-429 mimic in CEBPD-overexpressing BFTC909 and TCCSUP. Nevertheless, the inhibited regulation of hsa-miR-429 mimic on the expression of VEGFA and ability of HUVECs tube formation was rescued by the combined incubation with hsa-miR-429 inhibitor in these two UC-derived cell lines. Furthermore, the clinical correlations showed that the higher level of VEGFA or MVD has a positive correlation with the expression of CEBPD and a negative relation to hsa-miR-429 and leads to tumor aggressiveness with worse disease-specific, metastasis-free survival in UBUC and UTUC cohorts. Conclusions: We decipher the oncogenic mechanism of CEBPD on angiogenesis through the hsa-miR-429 inhibition to stabilize the expression of VEGFA in UC. The novel research unveiled the modulation of the CEBPD/hsa-miR-429/VEGFA axis on the progression of UC and could be accessible to theranostic biomarkers.

Keywords: CEBPD; hsa-miR-429; VEGFA; urothelial carcinoma; angiogenesis



Citation: Chan, T.-C.; Hsing, C.-H.; Shiue, Y.-L.; Huang, S.K.; Hsieh, K.-L.; Kuo, Y.-H.; Li, C.-F.

Angiogenesis Driven by the CEBPD–hsa-miR-429–VEGFA Signaling Axis Promotes Urothelial Carcinoma Progression. *Cells* **2022**, *11*, 638. <https://doi.org/10.3390/cells11040638>

Academic Editor: Marcello Tucci

Received: 17 January 2022

Accepted: 9 February 2022

Published: 11 February 2022

Publisher's Note: MDPI stays neutral with regard to jurisdictional claims in published maps and institutional affiliations.



Copyright: © 2022 by the authors. Licensee MDPI, Basel, Switzerland. This article is an open access article distributed under the terms and conditions of the Creative Commons Attribution (CC BY) license (<https://creativecommons.org/licenses/by/4.0/>).

1. Introduction

More than 90–95% of urothelial carcinoma (UC, also known as transitional cell carcinoma) emerge in bladder urothelial carcinoma (UBUC), and less than 10% of UC originate in upper tract urothelial carcinoma (UTUC, renal pelvis and ureter) in the United States [1]. Nevertheless, a higher prevalence of UTUC exists in Taiwan than in Western countries on account of the widespread use of aristolochic acid (AA) in traditional Chinese herbology before it was identified as a carcinogen for the development of kidney disease and UTUC [2,3]. UBUC was ranked as the tenth most commonly diagnosed malignancy, with 573,000 new cases and 213,000 deaths worldwide according to the estimation of the World Health Organization (WHO) [4]. For classification, UBUC can be categorized into papillary urothelial neoplasm of low malignant potential (PUNLMP), low-grade papillary UC and high-grade papillary UC based on cellular morphology in the grading system [5]. In the American

Joint Committee on Cancer (AJCC) TNM (tumor, node, metastasis) staging system, UBUC is defined as non-muscle-invasive bladder cancer (NMIBC) including carcinoma in situ (CIS or Tis), Ta, T1 and muscle-invasive bladder cancer (MIBC) comprising T2, T3, T4, due to its capacity of muscular aggressiveness [6].

NMIBC accounts for approximately 75% of UBUC and is characterized by a favorable survival rate but high recurrence and potential MIBC progression [7]. The standard management of NMIBC is transurethral resection, intravesical chemotherapy and immunotherapy with Bacillus Calmette–Guérin (BCG) [8]. MIBC is more advanced and requires multimodality treatment combined with chemotherapy, radical cystectomy and radical radiotherapy [9]. Notwithstanding aggressive management, over 50% of patients with MIBC are prone to proceed to metastasis with a survival time of 13 to 20 months [7]. Accordingly, a widespread understanding of the molecular signaling mechanism regulating UC to develop innovative biomarkers is imperative and beneficial to optimize cure options and avoid inferior clinical outcomes.

In our published research, we showed that the regulation of CEBPD (CCAAT/enhancer-binding protein delta) on tumor growth is partially through the transcriptional suppression of hsa-miR-429 to promote glycolysis-related HK2 expression in UTUC- and UBUC-derived cell lines (BFTC909, TCCSUP) [10]. CEBPD, a transcription factor that belongs to the CCAAT/enhancer-binding protein family, is not only involved in various normal biological processes including cell proliferation, differentiation, metabolism, immune responses, growth arrest and cell death [11,12] but also displays as a dual functional modulator to diminish or provoke cancer development [13–15]. hsa-miR-429, a member of the miR-200 family, functions as a tumor suppressor or oncomiR, depending on different types of cancer [16]. Our previous study exhibited that hsa-miR-429 is greatly expressed in the clinical specimens with aggressive UBUC and along with low survival rate in patients with UTUC and UBUC. Therefore, it is worthwhile to deeply explore alternative mediation of the CEBPD–hsa-miR-429 axis to shed light on underlying molecular mechanisms of UC progression.

Several genes that refer to carcinogenesis have been verified as the targets for hsa-miR-429 (Wang et al., 2019). VEGFA could be a possible target for hsa-miR-429 through the computational algorithm prediction ([10], Table S1). VEGFA belongs to the VEGF family (vascular endothelial growth factor; VEGFA, VEGFB, VEGFC, VEGFD, placenta growth factor [PGF]) and represents the best characteristics for angiogenesis to promote tumor growth and systemic metastasis (Carmeliet and Jain, 2011; Peach et al., 2018). Recently, CEBPD has been manifested to attribute chemotherapy-triggered angiogenesis to VEGF correlation and confer metastasis of lung cancer (Riedel et al., 2004; Chi et al., 2021), but the underlying mechanism is not yet well addressed. Accordingly, the study aimed to decipher the crosstalk of the CEBPD–hsa-miR-429–VEGFA axis on angiogenesis related to the progress of bladder cancer.

2. Materials and Methods

2.1. Cell Culture

Human UTUC- and UBUC-derived cell lines, namely BFTC909 and TCCSUP, respectively, were used in this study. BFTC909 was purchased from Food Industry Research and Development (FIRDI, Zhongzheng, Taipei, Taiwan), while TCCSUP was bought from American Type Tissue Culture Collection (American Type Culture Collection [ATCC], Manassas, VA, USA). Both BFTC909 and TCCSUP were maintained in the DMEM (Dulbecco's Modified Eagle Medium) with 10% FBS (fetal bovine serum), 1% P/S (Penicillin–Streptomycin) and was incubated in a 37 °C humidified incubator with 5% CO₂. Medium, serum and antibiotics were ordered from Gibco (Waltham, MA, USA).

2.2. Exogenous CEBPD Overexpression in BFTC909 and TCCSUP

Phoenix-AMPHO cell line (American Type Culture Collection [ATCC], Manassas, VA, USA) was used for the production of lentiviral particles containing the *CEBPD* gene. Briefly,

a mixture including viral vector for *CEBPD*, *psPAX2* (lentiviral packaging plasmid), *pMD2.G* (lentiviral envelope plasmid) purchased from National Core Facility for Biopharmaceuticals (NCFB, Nangang, Taipei, Taiwan) and PolyJet™ transfection reagents (SignaGen® Laboratories, Frederick, MD, USA) diluted in the Opti-MEM® I Reduced-Serum Medium (Gibco, Waltham, MA, USA) was delivered into Phoenix-AMPHO cells. After 48 h post-transfection, the viral supernatant was harvested and infected BFTC909 and TCCSUP. The UC cell lines with *CEBPD* overexpression were selected as stable clones after the incubation of the growth medium with 2 µg/mL puromycin (Gibco, Waltham, MA, USA).

2.3. Transfection of *hsa-miR-429* Mimic and Inhibitor

miRIDIAN microRNA Mimic Negative Control, miRIDIAN microRNA Human *hsa-miR-429* mimic and miRIDIAN microRNA Human *hsa-miR-429* inhibitor were all purchased from Horizon Discovery Group plc (Waterbeach, Cambridge, UK). miRIDIAN microRNA Human *hsa-miR-429* inhibitor is a synthetically single-strand inhibitor made up of chemically enhanced RNA oligonucleotides designed to bind and to sequester the complementary, mature *hsa-miR-429* strand. miRNAs were transfected into cells by using jetPRIME® in vitro DNA and siRNA transfection reagent (Polyplus-transfection SA, Illkirch-Grattenstaden, France). Concisely, 50 nM of miRNA Mimic Negative Control or *hsa-miR-429* mimic or inhibitor was diluted in the jetPRIME® buffer and was mixed with jetPRIME® reagent for 10 min at room temperature. After that, the transfection mix mentioned above was added to the cells with a fresh medium. Further experiments were executed after 72 h post-transfection.

2.4. Total RNA Isolation and Evaluation by Real-Time Quantitative RT-PCR

Total RNA was isolated from BFTC909 and TCCSUP by using Quick-RNA™ Miniprep Kit (Zymo Research, Irvine, CA, USA) according to the manufacturer's instructions. A proper amount of RNA was applied for cDNA synthesis by utilizing the Maxima First Strand cDNA Synthesis Kit referring to its manual (Gibco, Waltham, MA, USA) in a thermal cycler (Takara, Shiga, Japan). cDNA was mixed with predesigned TaqMan assay probe (*VEGFA* (Hs00900055_mL), Applied Biosystems; *POLR2A*, TopGen, Kaohsiung, Taiwan), using TaqMan Fast Advanced Master Mix (Thermo Scientific, Waltham, MA, USA) and was subjected to a StepOne Plus System machine to conduct quantitative RT-PCR for the mRNA level evaluation under $2^{-\Delta\Delta CT}$ formula. The data were shown as the fold change in *VEGFA* gene expression in the experimental group normalized to the *POLR2A* and relative to the control group.

2.5. Immunoblotting Assay

Total protein was isolated from BFTC909 and TCCSUP by using PRO-PREP Protein Extraction Solution (iNtRON Biotechnology, Seongnam, Korea) according to its manual. A proper amount of proteins was separated dependent on their molecular weight in a Bis-Tris Precast Gel (Merck Millipore, Burlington, MA, USA) and was transferred onto an Immobilon-P PVDF membrane (Merck Millipore, Burlington, MA, USA). The PVDF membrane (Merck Millipore, Burlington, MA, USA) was blocked with skim milk (MilliporeSigma, Burlington, MA, USA) followed by the incubation of anti-*VEGFA* primary antibody (ab214424, Abcam, Cambridge, UK) or anti-GAPDH primary antibody (ab181602, Abcam, Cambridge, UK) diluted with 5% milk in TBST. After washing, the membrane was incubated with 5% milk in TBST containing HRP Donkey anti-rabbit IgG (BioLegend®, San Diego, CA, USA). Afterward, the *VEGFA* or GAPDH protein was visualized by using enhanced chemiluminescence (ECL; Thermo Scientific).

2.6. Luciferase Reporter Assays

pMIR-REPORT-*VEGFA*-WT-3'UTR or pMIR-REPORT-*VEGFA*-mir-429-3p-mutant-3'UTR (Firefly luciferase reporter, TopGen) was co-transfected with pGL4.74[hRluc/TK] (Renilla luciferase reporter as internal control, Promega, Madison, WI, USA) into cells. After

72 h of incubation, the relative light units were detected by using Dual-Glo[®] Luciferase Assay System (Promega) with an ELISA reader (Promega, Madison, WI, USA). Firefly luciferase luminescence was normalized to Renilla luciferase luminescence to express the activity of WT or mutant VEGFA-3'UTR reporter.

2.7. HUVECs Tube Formation Assay

HUVEC (Human umbilical vein endothelial cell) was used for the tube formation assay. Concisely, Matrigel[®] Basement Membrane Matrix (Corning, Corning, NY, USA) was loaded into each inner well of the μ -Slide Angiogenesis (Ibidi, Fitchburg, WI, USA) and put in the 37 °C cell culture incubator for 30 min. Then 50 μ L cell suspension containing 7×10^3 cells in 25 μ L endothelial cell medium (ECM) with 2% FBS and 25 μ L conditioned medium was seeded into each well of μ -Slide. After 5 h of incubation, the image of tube formation was photographed by phase-contrast microscopy.

2.8. Human Tumor Tissue Specimens

295 UBUC and 340 UTUC specimens from the biobank of Chi Mei Medical Center were used for the immunohistochemistry (IHC) and In Situ Hybridization Detection of miRNA. The archived tumor specimens were obtained from surgery with curative intent between January 1996 and May 2004 as our previous study described [17]. This research was approved by the institutional review board of Chi Mei Medical Center (IRB10207-001).

2.9. Immunohistochemistry (IHC)

Paraffin-embedded (FFPE) blocks of the clinical sample were microdissected (4 μ m) and put onto precoated slides. Wax melting of the slides was conducted in a 65 °C oven for 20 min. After that, slides were deparaffinized with xylene and rehydrated with ethanol from high concentration to low concentration (100%, 95%, 75%) and distilled water, sequentially. The antigen retrieval process was treated with citrate buffer (10 mM citric acid, pH 6) in a microwave oven for 20 min. After cooling, endogenous peroxidase of slides was eliminated with Peroxidase-Blocking Solution (Dako, Glostrup, Hovedstaden, Denmark), followed by the incubation of the indicated primary antibody (CEBPD, NB110-85519; VEGFA, ab214424; PECAM1, ab28364) for one hour at room temperature. After washing with PBS, slides were incubated with peroxidase-conjugated secondary antibody reagent (REAL[™] EnVision[™]/HRP, Rabbit/Mouse (ENV); Dako, Glostrup, Hovedstaden, Denmark) for 30 min at room temperature. The targeted protein was visualized with EAL[™] DAB+ Chromogen diluted in REAL[™] Substrate Buffer (Dako, Glostrup, Hovedstaden, Denmark). The nuclear location was detected with Gill's hematoxylin. Afterward, slides were dehydrated with ethanol (75%, 95% and 100%) and mounted. The image was captured by phase-contrast microscopy and examined by an expert pathologist (CF Li) in Chi Mei Medical Center (Tainan, Taiwan). Computerized analysis was performed to quantify tumoral microvessel density (MVD) of the PECAM1-labeled vessels by ImageJ software, which calculated the percentage of vessel areas in each representative field.

2.10. In Situ Hybridization Detection of miRNA Using LNA[™] Oligonucleotides

Hsa-miR429 was detected by the IsHyb In Situ Hybridization Kit (BioChain, Newark, CA, USA) according to its manufacturer's instructions. Concisely, after wax melting and deparaffinization as the IHC procedure mentioned above, slices were treated with 4% DEPC-paraformaldehyde followed by a wash with DEPC-PBS. Then samples were treated with Proteinase K and were washed with DEPC-PBS. Following the treatment with prehybridization solution, the slices were incubated with a digoxigenin-labeled LNA probe against hsa-miR-429 overnight. The slides were washed by 2X SSC, 1.5X SSC and 0.2X SSC once serially and were incubated with AP-conjugated anti-digoxigenin antibody. After that, the samples were incubated with a mixture of nitro-blue tetrazolium (NBT) and 5-bromo-4-chloro-3'-indolyphosphate (BCIP) diluted in 1X alkaline phosphatase buffer in the dark. The Nuclear Fast Red solution (MilliporeSigma, Burlington, MA, USA) was

applied for nuclear counterstaining. After the dehydration procedure with ethanol from low concentration to high concentration (75%, 95% and 100%), the slices were mounted and examined.

2.11. Statistics

Chi-square test, Spearman's rank correlation coefficient and the Mann–Whitney U test using SPSS software (version 14.0, IBM, Armonk, NY, USA) were utilized to estimate the associations and correlations between CEBPD, VEGFA, hsa-miR-429, MVD, clinicopathologic variables and the comparisons for several functional studies. The expression status of targeted proteins and hsa-miR-429 were evaluated in line with our previous works [10]. Disease-specific survival (DSS) and metastasis-free survival (MeFS) were estimated and plotted through log-rank tests and Kaplan–Meier curves, respectively. Independent prognostic impacts of selected parameters were estimated by a multivariate Cox proportional hazards model. Differences with a two-tailed p -value lower than 0.05 were considered significant for all analyses.

3. Results

3.1. hsa-miR-429 Inhibits the Expression of VEGFA and Angiogenesis in BFTC909 and TCCSUP by Directly Targeting VEGFA mRNA

Because downregulated hsa-miR-429 in CEBPD-overexpressing cell lines has been unveiled in our previous study [10], we next examine the correlation between CEBPD, hsa-miR-429 and VEGFA in UC cell lines. Figures 1 and 2 showed that the mRNA and protein level of VEGFA were promoted after exogenous CEBPD overexpression in BFTC909 and TCCSUP compared to those of the mock group. The treatment of hsa-miR-429 mimic diminished the capacity of CEBPD on the upregulation of VEGFA mRNA and protein expression. While the repressed mRNA and protein of VEGFA aroused from the hsa-miR-429 mimic in CEBPD-overexpressing cell lines were retrieved by the has-miR-429 inhibitor.

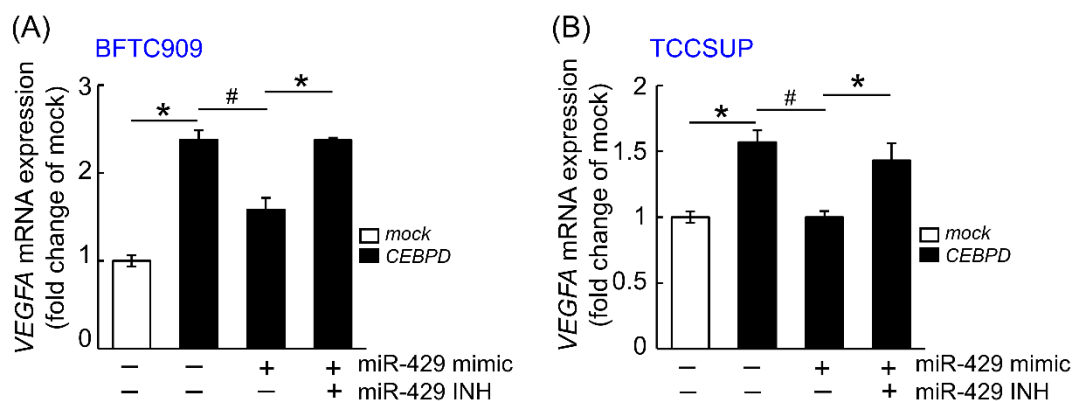


Figure 1. The inhibition effect of hsa-miR-429 mimic on VEGFA transcript is rescued after the combined treatment of hsa-miR-429 inhibitor in CEBPD-overexpressing BFTC909 and TCCSUP. Quantitative RT-PCR indicates that the mRNA level of VEGFA is evidently increased in the BFTC909 (A) and TCCSUP (B) cells with ectopic CEBPD expression than mock delivery. The transcript of VEGFA is significantly inhibited after the treatment of 50 nM hsa-miR-429 mimic for 72 h compared to that incubated of miRNA Mimic Negative Control in CEBPD-overexpressing cells. The combined transfection of hsa-miR-429 mimic (50 nM) and hsa-miR-429 inhibitor (50 nM) for 72 h recover the impact of CEBPD on the increase in the mRNA level of VEGFA in BFTC909 and TCCSUP cells. Data were executed in triplicate, and the statistical graphics are shown as the mean \pm SEM. Statistical significance: * # $p < 0.05$. * is for the significant upregulation while # is for the significant downregulation.

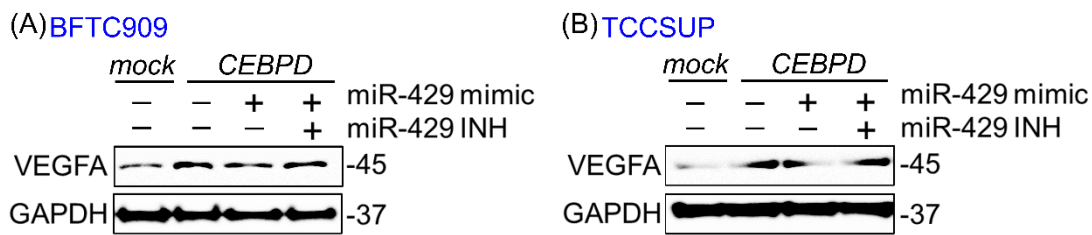


Figure 2. Downregulation of VEGFA protein expression by hsa-miR-429 mimic is rescued by the hsa-miR-429 inhibitor in the CEBPD-overexpressing BFTC909 and TCCSUP. Immunoblotting shows that the lentiviral-delivered CEBPD overexpression robustly promotes the protein level of VEGFA in BFTC909 (A) and TCCSUP (B) cells than in the mock-expressing cell lines. Upregulated VEGFA protein induced by the CEBPD is diminished after the transfection of 50 nM hsa-miR-429 mimic for 72 h in these two cells. A quantity of 50 nM hsa-miR-429 inhibitor could offset the depressing effect of 50 nM hsa-miR-429 mimic on the VEGFA protein in CEBPD-infected cells. GAPDH is served as a loading control.

To confirm if the *VEGFA* transcript is directly targeted by the hsa-miR-429, BFTC909 (Figure 3A) and TCCSUP (Figure 3B) cell lines were co-transfected with WT (wild type)- or mutant-*VEGFA* 3'-UTR firefly luciferase reporter and miRNA Mimic Negative Control or hsa-miR-429 mimic or both hsa-miR-429 mimic and inhibitor. The hsa-miR-429 mimic markedly inhibited the luciferase activity of the WT-*VEGFA* 3'-UTR compared to BFTC909 and TCCSUP with miRNA Mimic Negative Control. The decreasing luciferase activity of the WT-*VEGFA* 3'-UTR caused by hsa-miR-429 mimic was rescued after treating with the combination of hsa-miR-429 mimic and inhibitor in these two cell lines. However, the transfection of miRNA Mimic Negative Control, hsa-miR-429 mimic, the combination of hsa-miR-429 mimic and inhibitor all failed to affect the firefly luciferase activity once BFTC909 and TCCSUP were transfected with mutant-*VEGFA* 3'-UTR reporter. The above data assumed that hsa-miR-429 directly targets the *VEGFA* transcript to inhibit its mRNA and protein expression.

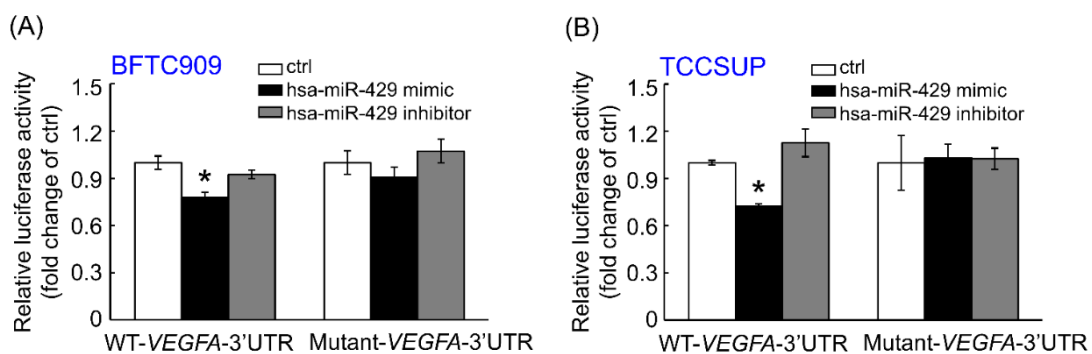


Figure 3. hsa-miR-429 regulates the expression of *VEGFA* transcript through targeting its 3'-UTR. The relative luciferase activity of wild type-*VEGFA*-3'-UTR reporter is strikingly decreased after the transfection of 50 nM hsa-miR-429 mimic for 72 h in both BFTC909 (A) and TCCSUP (B) cells compared to those of the control group. Nevertheless, the hsa-miR-429 mimic has no significant effect on the wild type-*VEGFA*-3'-UTR-Luc upon the presence of the 50 nM hsa-miR-429 inhibitor in these two cells. Furthermore, neither hsa-miR-429 mimic nor the combination of hsa-miR-429 mimic and inhibitor change the relative luciferase activity of mutant-*VEGFA*-3'-UTR in BFTC909 and TCCSUP. All data were conducted in triplicate and are represented as the mean \pm SEM. Statistical significance: * $p < 0.05$.

Given that VEGFA is a critical factor for the angiogenesis in cancers, the ability of HUVECs tube formation was determined in the mock-CEBPD-overexpressing BFTC909 and TCCSUP cells treated with miRNA mimic negative control or hsa-miR-429 mimic

or/and hsa-miR-429 inhibitor. Figure 4 shows that conditioned medium from the CEBPD-overexpressing BFTC909 and TCCSUP notably enhanced HUVECs tube formation compared to those from the mock group. Nevertheless, the ability of HUVEC-based tube formation was hampered after the treatment of conditioned medium from the CEBPD-overexpressing BFTC909 and TCCSUP transfected with hsa-miR-429 mimic than those from the UC-derived cells with CEBPD overexpression, while it was rescued upon treating with medium collected from transfecting hsa-miR-429 mimic and inhibitor simultaneously to ectopic CEBPD overexpression cells.

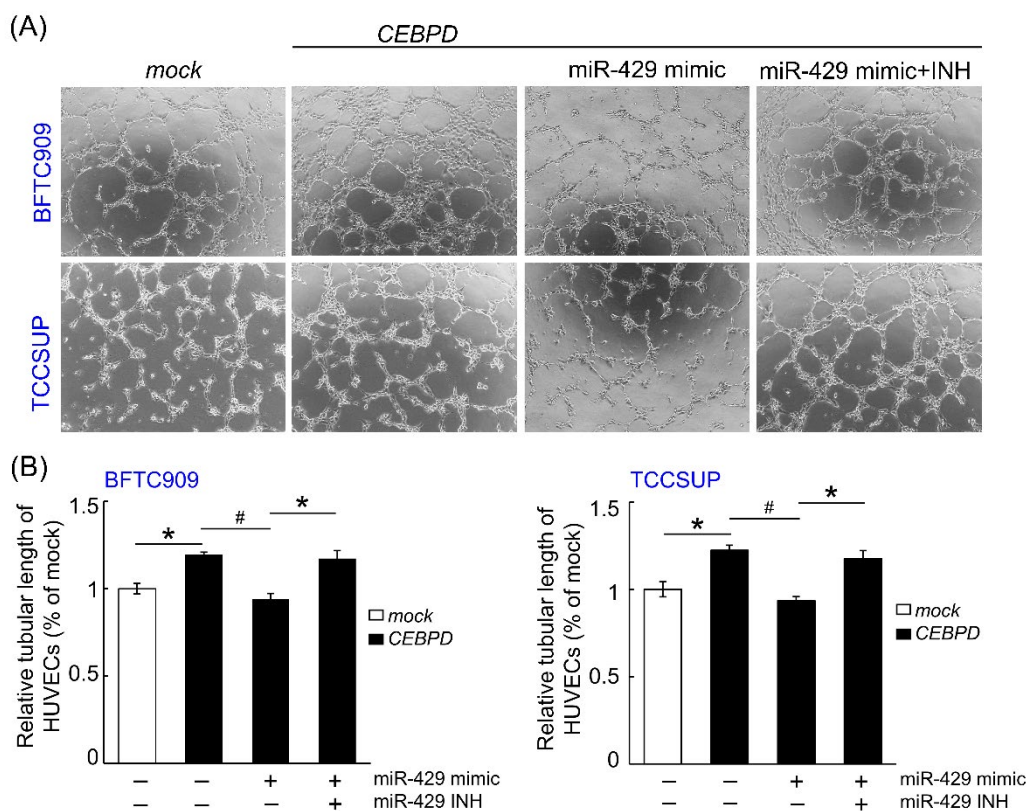


Figure 4. CEBPD overexpression-induced HUVEC tube forming in BFTC909 and TCCSUP is restrained by hsa-miR-429 mimic and is rescued by has-miR-429 inhibitor. (A) The ability of tube formation is markedly increased when the HUVECs are incubated with the conditioned medium from the CEBPD-overexpressing BFTC909 and TCCSUP than from the mock-groups. Nevertheless, conditioned medium from the CEBPD-overexpressing cells after the transfection of 50 nM hsa-miR-429 mimic for three days destroys the capacity of HUVECs tube formation. However, the conditioned medium collected from the BFTC909 and TCCSUP transfected with combined 50 nM hsa-miR-429 mimic and inhibitor for 3 days resists the repressed effect of the hsa-miR-429 mimic transfection alone on HUVECs tube forming. The statistical data are shown in (B). All experimental data were proceeded in triplicate and are shown as the mean \pm SEM. Statistical significance: * # $p < 0.05$. * is for the significant upregulation while # is for the significant downregulation.

3.2. UBUC and UTUC Patients with High Expression of VEGFA and High Microvascular Density Are Usually Accompanied by Higher CEBPD Expression, Lower hsa-miR-429 and Inferior Survival Outcomes

Aside from in vitro research, we then investigated the correlations between CEBPD, hsa-miR-429 and VEGFA expression and their associations with microvascular density and clinical aggressiveness in UBUC and UTUC cohorts comprised of cancer tissue samples from 295 and 340 patients, respectively. Of note, CEBPD high expression positively correlated with higher VEGFA expression and more PECAM1-labeled MVD and negatively correlated with hsa-miR-429 in both UBUC and UTUC (Figure 5). Moreover, it turned out

that higher expression of CEBPD, VEGFA and PECAM1-labeled MVD but lower levels of hsa-miR-429 were associated with numerous adverse clinicopathological factors. UBUCs and UTUCs with high expression of VEGFA usually have a positive correlation with high pathological staging (T, $p < 0.001$ and $p < 0.001$), high nodal metastasis ($p < 0.001$ and $p < 0.001$), high histological grade ($p < 0.001$ and $p = 0.015$), the presence of vascular invasion ($p < 0.001$ and $p < 0.001$) and perineural invasion ($p < 0.001$ and $p < 0.001$), high mitotic rate ($p < 0.001$ and $p = 0.022$) and high CEBPD expression ($p < 0.001$ and $p < 0.001$) but less hsa-miR-429 expression ($p < 0.001$ and $p < 0.001$) (Tables 1 and 2). Similarly, high microvascular density is also accompanied by high pathological staging (T, $p < 0.001$ and $p < 0.001$, high nodal metastasis ($p < 0.001$ and $p < 0.001$), high histological grade ($p < 0.001$ and $p < 0.001$), the presence of vascular invasion ($p < 0.001$ and $p = 0.001$), perineural invasion ($p < 0.001$ and $p < 0.001$), high CEBPD expression ($p < 0.001$ and $p < 0.001$) (Figure 6A,D), high VEGFA expression ($p < 0.001$ and $p < 0.001$) (Figure 6B,E) and low level of hsa-miR-429 ($p < 0.001$ and $p < 0.001$) (Figure 6C,F) in both UBUC and UTUC (Tables 1 and 2). However, high microvascular density was only evidently related to high mitotic rate in UTUC ($p = 0.005$) while being marginally correlated in UBUC ($p = 0.138$) (Tables 1 and 2). Furthermore, the univariate analysis indicated that disease-specific survival (DSS) and metastasis-free survival (MeFS) were negatively determined by aggressive pT status (T), the presence of nodal metastasis, higher histological grade, the presence of vascular invasion and perineural invasion, higher expression of CEBPD and VEGFA (Figure 7A,B,E,F) and higher microvascular density (Figure 7C,D,G,H) in UBUC and UTUC. Yet, the lower expression of hsa-miR-429 confers a better prognosis. Moreover, DSS and MeFS represented a relation to high mitotic rate only in UBUC instead of UTUC patients under univariate analysis (Tables 3 and 4). In multivariate analysis, UBUCs with high pT status ($p = 0.003$, R.R. = 12.308), high mitotic rate ($p = 0.026$, R.R. = 2.173) and high microvascular density ($p = 0.021$, R.R. = 3.509) showed significant worse DSS. The higher mitotic count ($p = 0.036$, R.R. = 1.721) and higher microvascular density ($p < 0.001$, R.R. = 11.494) were the most significant determinants for worse MeFS (Table 3). For UTUC, those with the presence of multifocality ($p = 0.001$, R.R. = 2.748), nodal metastasis ($p < 0.001$, R.R. = 3.802), perineural invasion ($p = 0.009$, R.R. = 2.799) and microvascular density ($p = 0.003$, R.R. = 4.596) had deteriorated DSS. The multivariate survival analysis for MeFS disclosed numerous factors including multifocality ($p = 0.002$, R.R. = 2.488), higher primary tumor status ($p = 0.050$, R.R. = 3.731), vascular invasion ($p = 0.010$, R.R. = 2.346), higher CEBPD ($p < 0.001$, R.R. = 3.886) and higher microvascular density ($p = 0.001$, R.R. = 5.611), which are significant independent survival determinants. The above data disclosed that the high status of CEBPD, VEGFA and microvascular density along with a low level of hsa-miR-429 strongly associated with aggressiveness and adverse survival rate.

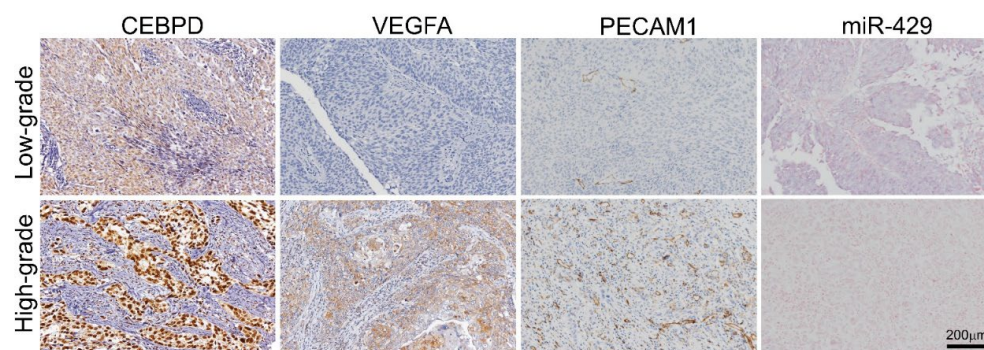


Figure 5. Higher expression of CEBPD is associated with lower hsa-miR-429, higher VEGFA expression, higher PECAM1-labeled microvascular density (MVD) and higher histological grade in UC. Immunohistochemistry shows that a higher level of CEBPD is associated with lower hsa-miR-429 expression. Of note, CEBPD expression is also correlated with high VEGFA expression, high PECAM1-labeled MVD and high histological grade in UC.

Table 1. Correlations between CEBPD, miR-429 and VEGFA expression, microvascular density and other important clinicopathological parameters in UBUC.

| Parameter | Category | Case No. | VEGFA Expression | | | Microvascular Density | | |
|---|------------------|----------|------------------|--------------|----------|-----------------------|--------------|----------|
| | | | Low | High | p Value | Low | High | p Value |
| Sex & | Male | 216 | 111 | 105 | 0.376 | 108 | 108 | 0.923 |
| | Female | 79 | 36 | 43 | | 39 | 40 | |
| Age (years) & | <65 | 121 | 60 | 61 | 0.944 | 61 | 60 | 0.867 |
| | ≥65 | 174 | 87 | 87 | | 86 | 88 | |
| Primary tumor (T) & | Ta | 84 | 70 | 14 | <0.001 * | 73 | 11 | <0.001 * |
| | T1 | 88 | 51 | 37 | | 51 | 37 | |
| | T2–T4 | 123 | 26 | 97 | | 23 | 100 | |
| Nodal metastasis & | Negative (N0) | 266 | 143 | 123 | <0.001 * | 147 | 119 | <0.001 * |
| | Positive (N1–N2) | 29 | 4 | 25 | | 0 | 29 | |
| Histological grade & | Low grade | 56 | 46 | 10 | <0.001 * | 43 | 13 | <0.001 * |
| | High grade | 239 | 101 | 138 | | 104 | 135 | |
| Vascular invasion & | Absent | 246 | 140 | 106 | <0.001 * | 140 | 106 | <0.001 * |
| | Present | 49 | 7 | 42 | | 7 | 42 | |
| Perineural invasion & | Absent | 275 | 145 | 130 | <0.001 * | 145 | 130 | <0.001 * |
| | Present | 20 | 2 | 18 | | 2 | 18 | |
| Mitotic rate (per 10 high power fields) # | | 295 | 11.3 ± 14.12 | 17.5 ± 13.30 | <0.001 * | 13.2 ± 15.64 | 15.6 ± 12.18 | 0.138 |
| CEBPD expression & | Low expression | 207 | 140 | 67 | <0.001 * | 144 | 63 | <0.001 * |
| | High expression | 88 | 7 | 81 | | - | 3 | |
| miR-429 expression & | High expression | 194 | 64 | 130 | <0.001 * | 66 | 128 | <0.001 * |
| | Low expression | 101 | 83 | 18 | | 81 | 20 | |
| VEGFA expression & | Low expression | 147 | - | - | - | 120 | 27 | <0.001 * |
| | High expression | 148 | - | - | | - | 27 | |

& Chi-square test; # Mann–Whitney U test; all other comparisons; * Statistical significance. Tumor samples were taken from the biobank of Chi Mei Medical Center.

Table 2. Correlations between CEBPD, miR-429 and VEGFA expression, microvascular density and other important clinicopathological parameters in UTUC.

| Parameter | Category | Case No. | VEGFA Expression | | | Microvascular Density | | |
|---|------------------|----------|------------------|--------------|----------|-----------------------|---------------|----------|
| | | | Low | High | p Value | Low | High | p Value |
| Sex & | Male | 158 | 76 | 82 | 0.514 | 76 | 82 | 0.514 |
| | Female | 182 | 94 | 88 | | 94 | 88 | |
| Age (years) & | <65 | 138 | 80 | 58 | 0.015 * | 77 | 61 | 0.077 |
| | ≥65 | 202 | 90 | 112 | | 93 | 109 | |
| Multifocality & | Single | 278 | 145 | 133 | 0.092 | 141 | 137 | 0.574 |
| | Multifocal | 62 | 25 | 37 | | 29 | 33 | |
| Primary tumor (T) & | Ta | 89 | 68 | 21 | <0.001 * | 70 | 19 | <0.001 * |
| | T1 | 92 | 61 | 31 | | 63 | 29 | |
| | T2–T4 | 159 | 41 | 118 | | 37 | 122 | |
| Nodal metastasis & | Negative (N0) | 312 | 168 | 144 | <0.001 * | 168 | 144 | <0.001 * |
| | Positive (N1–N2) | 28 | 2 | 26 | | 2 | 26 | |
| Histological grade & | Low grade | 56 | 42 | 14 | 0.015 * | 40 | 16 | <0.001 * |
| | High grade | 284 | 128 | 156 | | 130 | 154 | |
| Vascular invasion & | Absent | 234 | 150 | 84 | <0.001 * | 157 | 77 | 0.001 * |
| | Present | 106 | 20 | 86 | | 13 | 93 | |
| Perineural invasion & | Absent | 321 | 169 | 152 | <0.001 * | 169 | 152 | <0.001 * |
| | Present | 19 | 1 | 18 | | 1 | 18 | |
| Mitotic rate (per 10 high power fields) # | | 340 | 10.8 ± 12.02 | 13.8 ± 12.38 | 0.022 * | 10.5 ± 11.58 | 14.16 ± 12.71 | 0.005 * |
| CEBPD expression & | Low expression | 251 | 158 | 93 | <0.001 * | 153 | 98 | <0.001 * |
| | High expression | 89 | 12 | 77 | | 17 | 72 | |
| miR-429 expression & | High expression | 257 | 109 | 148 | <0.001 * | 113 | 144 | <0.001 * |
| | Low expression | 83 | 61 | 22 | | - | 57 | |
| VEGFA expression & | Low expression | 170 | - | - | - | 129 | 41 | <0.001 * |
| | High expression | 170 | - | - | | 41 | 129 | |

& Chi-square test; # Mann–Whitney U test; * Statistical significance. Tumor samples were taken from the biobank of Chi Mei Medical Center.

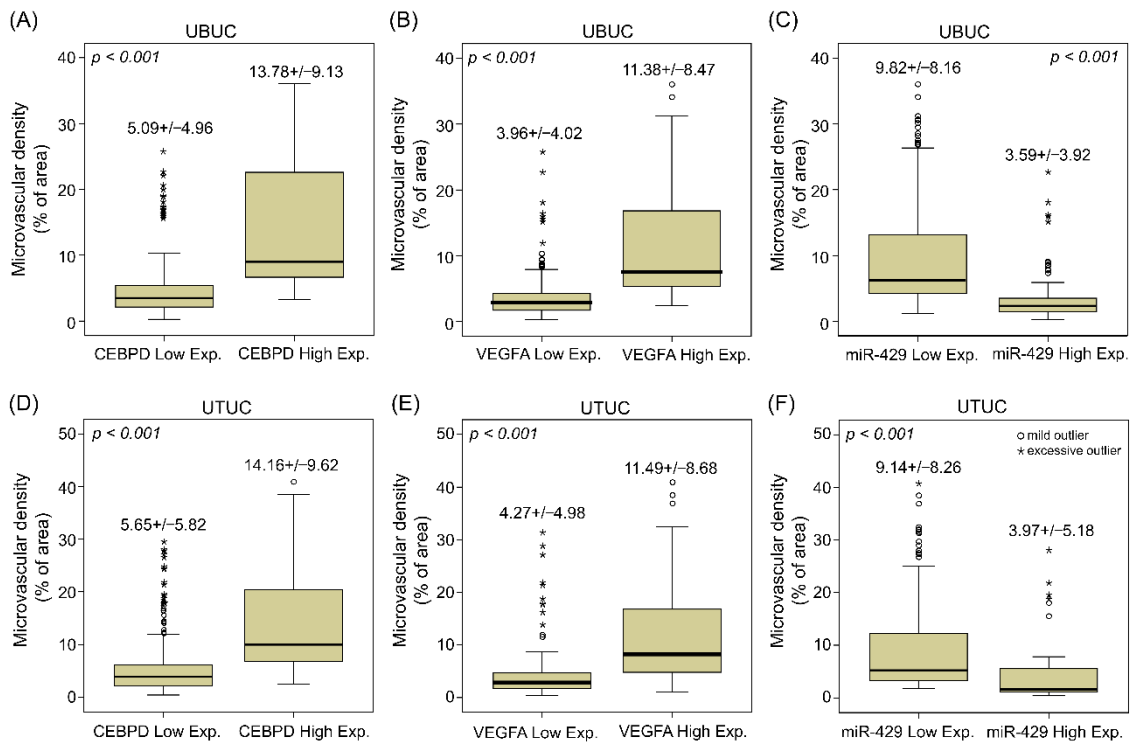


Figure 6. The expression of CEBPD and VEGFA have a positive correlation, but hsa-miR-429 represents a negative relation with MVD in UBC and UTUC. Microvascular density is quantified by computerizing PECAM1-labeled vessels from IHC staining in UBC and UTUC specimens using ImageJ software, which evaluated the proportion of vascular field in each representative area. Quantitative results show the UBC and UTUC samples with higher CEBPD (A,D) and VEGFA (B,E), but lower levels of hsa-miR-429 (C,F) tend to have higher MVD. A circle symbol indicates a mild outlier (1.5 box lengths from the hinge of the box), and an asterisk is used to point an excessive outlier (3 box lengths from the hinge of the box).

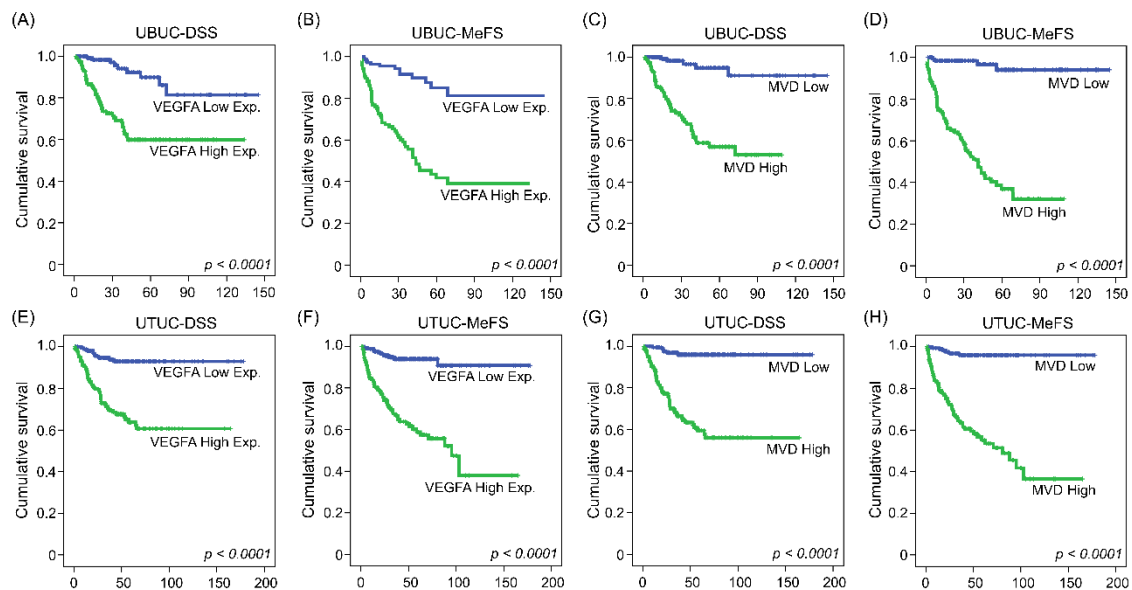


Figure 7. High expression of VEGFA and MVD are correlated with inferior survival outcomes in UBC and UTUC patients. Kaplan–Meier plot examined that a higher level of VEGFA or MVD confers deteriorated clinical outcomes in terms of disease-specific survival and metastatic-free survival in patients with UBC (A–D) and UTUC (E–H).

Table 3. Univariate log-rank and multivariate analyses for disease-specific and metastasis-free survival in UBC.

| Parameter | Category | Case No. | Disease-Specific Survival | | | | | Metastasis-Free Survival | | | | |
|--|------------------|----------|---------------------------|-----------|-----------------------|---------------|---------|--------------------------|-----------|-----------------------|--------------|---------|
| | | | Univariate Analysis | | Multivariate Analysis | | | Univariate Analysis | | Multivariate Analysis | | |
| | | | No. of Events | p Value | RR | 95% CI | p Value | No. of Events | p-Value | RR | 95% CI | p Value |
| Sex | Male | 216 | 41 | 0.4906 | - | - | - | 61 | 0.2745 | - | - | - |
| | Female | 79 | 11 | | - | - | - | 16 | | - | - | - |
| Age (years) | <65 | 121 | 17 | 0.1315 | - | - | - | 32 | 0.8786 | - | - | - |
| | ≥65 | 174 | 35 | | - | - | - | 45 | | - | - | - |
| Primary tumor (T) | Ta | 84 | 1 | <0.0001 * | 1 | - | 0.003 * | 4 | <0.0001 * | 1 | - | 0.491 |
| | T1 | 88 | 9 | | 3.532 | 0.343–36.331 | | 23 | | 2.126 | 0.533–8.176 | |
| | T2–T4 | 123 | 42 | | 12.308 | 1.194–126.906 | | 50 | | 2.344 | 0.576–9.529 | |
| Nodal metastasis | Negative (N0) | 266 | 41 | 0.0001 * | 1 | - | 0.923 | 61 | <0.0001 * | 1 | - | 0.123 |
| | Positive (N1–N2) | 29 | 11 | | 1.036 | 0.507–2.115 | | 16 | | 1.614 | 0.878–2.966 | |
| Histological grade | Low grade | 56 | 2 | 0.0016 * | 1 | - | 0.809 | 5 | 0.0007 * | 1 | - | 0.576 |
| | High grade | 239 | 50 | | 0.814 | 0.153–4.326 | | 72 | | 1.363 | 0.460–4.039 | |
| Vascular invasion | Absent | 246 | 37 | 0.0010 * | 1 | - | 0.108 | 54 | <0.0001 * | 1 | - | 0.726 |
| | Present | 49 | 15 | | 0.558 | 0.274–1.137 | | 23 | | 0.898 | 0.492–1.640 | |
| Perineural invasion | Absent | 275 | 44 | <0.0001 * | 1 | - | 0.065 | 67 | 0.0003 * | 1 | - | 0.311 |
| | Present | 20 | 8 | | 2.252 | 0.952–5.327 | | 10 | | 1.491 | 0.689–3.227 | |
| Mitotic rate(per 10 high power fields) | <10 | 139 | 12 | 0.0001 * | 1 | - | 0.026 * | 23 | <0.0002 * | 1 | - | 0.036 * |
| | ≥10 | 156 | 40 | | 2.173 | 1.097–4.304 | | 54 | | 1.721 | 1.035–2.864 | - |
| CEBPD expression | Low | 207 | 22 | <0.0001 * | 1 | - | 0.259 | 32 | <0.0001 * | 1 | - | 0.452 |
| | High | 88 | 30 | | 1.446 | 0.762–2.742 | | 45 | | 1.216 | 0.730–2.026 | |
| miR-429 expression | Low | 194 | 48 | <0.0001* | 1 | - | 0.273 | 66 | <0.0001 * | 1 | - | 0.987 |
| | High | 101 | 4 | | 0.542 | 0.182–1.618 | | 11 | | 1.006 | 0.499–2.026 | |
| VEGFA expression & | Low expression | 147 | 9 | <0.0001 * | - | - | 0.980 | 13 | <0.0001 * | - | - | 0.258 |
| | High expression | 148 | 43 | | 1.012 | 0.414–2.471 | | 64 | | 1.501 | 0.742–3.035 | - |
| Microvascular density | Low | 147 | 5 | <0.0001 * | 1 | - | 0.021 * | 4 | <0.0001 * | 1 | - | <0.001 |
| | High | 148 | 47 | | 3.509 | 1.208–10.196 | | 73 | | 11.494 | 3.825–34.542 | |

& Chi-square test; * Statistical significance.

Table 4. Univariate log-rank and multivariate analyses for disease-specific and metastasis-free survival in UTUC.

| Parameter | Category | Case No. | Disease-Specific Survival | | | | | Metastasis-Free Survival | | | | |
|--|------------------|----------|---------------------------|-----------|-----------------------|--------------|----------|--------------------------|-------------|-----------------------|--------------|----------|
| | | | Univariate Analysis | | Multivariate Analysis | | | Univariate Analysis | | Multivariate Analysis | | |
| | | | No. of Events | p Value | RR | 95% CI | p Value | No. of Events | p Value | RR | 95% CI | p Value |
| Sex | Male | 158 | 28 | 0.9301 | - | - | - | 32 | 0.7904 | - | - | - |
| | Female | 182 | 33 | | - | - | - | 38 | | - | - | - |
| Age (years) | <65 | 138 | 26 | 0.8660 | - | - | - | 30 | 0.8470 | - | - | - |
| | ≥65 | 202 | 35 | | - | - | - | 40 | | - | - | - |
| Multifocality | Single | 273 | 43 | 0.0042 * | 1 | - | 0.001 * | 52 | 0.0196 * | 1 | - | 0.002 * |
| | Multifocal | 62 | 18 | | 2.748 | 1.516–4.984 | | 18 | | 2.488 | 1.175–3.665 | |
| Primary tumor (T) | Ta | 89 | 2 | <0.0001 * | 1 | - | 0.088 | 4 | <0.0001 * | 1 | - | 0.050 * |
| | T1 | 92 | 9 | | 3.642 | 0.726–18.220 | | 15 | | 1.924 | 0.580–6.378 | |
| | T2–T4 | 159 | 50 | | 4.162 | 0.877–19.757 | | 51 | | 3.731 | 1.141–12.197 | |
| Nodal metastasis | Negative ((N0) | 312 | 42 | <0.0001 * | 1 | - | <0.001 * | 55 | <0.0001 * | 1 | - | 0.104 |
| | Positive (N1–N2) | 28 | 19 | | 3.802 | 1.998–7.234 | | 15 | | 1.711 | 0.895–3.271 | |
| Histological grade | Low grade | 56 | 4 | 0.0171 * | 1 | - | 0.105 | 3 | 0.0019 * | 1 | - | 0.398 |
| | | | | | 2.580 | 0.820–8.122 | | 1.733 | 0.484–6.206 | | | |
| Vascular invasion | Absent | 234 | 24 | <0.0001 * | 1 | - | 0.458 | 26 | <0.0001 * | 1 | - | 0.010 * |
| | Present | 106 | 37 | | 1.268 | 0.677–2.376 | | 44 | | 2.346 | 1.231–4.469 | |
| Perineural invasion | Absent | 321 | 50 | <0.0001 * | 1 | - | 0.009 * | 61 | <0.0001 * | 1 | - | 0.238 |
| | Present | 19 | 11 | | 2.799 | 1.296–6.048 | | 9 | | 1.599 | 0.733–3.487 | |
| Mitotic rate(per 10 high power fields) | <10 | 173 | 27 | 0.1268 | - | - | - | 30 | 0.0581 | - | - | - |
| | ≥10 | 167 | 34 | | - | - | - | 40 | | - | - | - |
| CEBPD expression | Low | 251 | 26 | <0.0001 * | 1 | - | 0.081 | 24 | <0.0001 * | 1 | - | <0.001 * |
| | High | 89 | 35 | | 1.740 | 0.934–3.243 | | 46 | | 3.886 | 2.119–7.125 | |
| miR-429 expression | Low | 257 | 55 | 0.0024 * | 1 | - | 0.908 | 64 | <0.0001 * | 1 | - | 0.633 |
| | High | 83 | 6 | | 1.055 | 0.423–2.633 | | 6 | | 1.250 | 0.500–3.127 | |
| VEGFA expression & | Low expression | 170 | 10 | <0.0001 * | - | - | 0.743 | 10 | <0.0001 * | - | - | 0.660 |
| | High expression | 170 | 51 | | 0.868 | 0.371–2.029 | | 60 | | 1.202 | .530–2.724 | |
| Microvascular density | Low | 170 | 6 | <0.0001 * | 1 | - | 0.003 * | 6 | <0.0001 * | 1 | - | 0.001 * |
| | High | 170 | 55 | | 4.596 | 1.666–12.679 | | 64 | | 5.611 | 2.102–14.976 | |

& Chi-square test; * Statistical significance.

4. Discussion

The novel correlation of the CEBPD–hsa-miR-429–VEGFA axis on UC angiogenesis and its important clinical significance were disclosed unprecedentedly in our present study. We discovered that CEBPD failed to increase the expression of VEGFA and capacity of HUVECs tube formation after the treatment of hsa-miR-429 mimic in BFTC909 and TCCSUP cell lines. However, hsa-miR-429 inhibitor could offset the depression of hsa-miR-429 mimic on mRNA expression of VEGFA and tube formation in CEBPD-overexpressing cells. Furthermore, UCs with the substantial expression of VEGFA and high microvascular density tended to be more aggressive and pursued worse clinical outcomes on account of the possession of higher expression of CEBPD and lower hsa-miR-429.

CEBPD is a well-known transcription factor and holds dual traits as a tumor suppressor in hepatocellular carcinoma [18], prostate cancer cells [19] or oncogene in lung adenocarcinoma [20], breast cancer [21] and UC [15] based on the diverse microenvironments of tumors [14,22–25]. In our previous study, we also fortified the oncogenic characteristic of CEBPD on UC specimens [10]. Owing to the multifaceted CEBPD of neoplasm, it is obligatory to excavate its widespread mechanism. To date, the reduction of MKI67 (cell proliferation marker) and PECAM1 (endothelial cell marker) has been observed in the *Cebpd*-deficient mice. Conditioned media incubated with *CEBPD*-knockdown cells also diminished the HUVECs tube formation [25], implying the vasculature development could be stimulated through the CEBPD expression.

miRNAs are pivotal for normal physiologic processes [26], while aberrant miRNAs are characterized as vital elements for tumor promotion or suppression depending on the different types of cancers [27]. hsa-miR-429 is a member of the hsa-miR-200 family. The loss of hsa-miR-429 mainly existed in the UBUCs with high grade and was strongly linked to adverse clinicopathological features and worse outcomes [28]. Consistently, a high level of hsa-miR-429 was detected in the low-grade UBUC cell line that inhibits cell invasion through the downregulation of proteins related to epithelial–mesenchymal transition (EMT) that enables tumor progression and metastasis [29]. Moreover, hsa-miR-429 was also depicted to act as an antimetastatic miRNA through the depletion of Raf/MEK/ERK-EMT pathway in hepatocellular carcinoma [30].

Administration of gemcitabine plus cisplatin is now considered as a first-line chemotherapy regimen for advanced or metastatic UC [31], but the prognostic outcome is still unsatisfactory, and the demand for combined remedy is pressing. Metastasis progression and nourishment supply strongly rely on vascularization in tumors [32]. VEGFA, a member of VEGF, binds to tyrosine kinase receptors (VEGFR-1 and VEGFR-2) and is a leading contributor to the formation of new blood vessels and promotes vascular permeability [33,34]. In cancer, VEGFA mainly comes from endothelial cells, hypoxic tumor cells and tumor-associated macrophages [35]. VEGFA-modulated neoangiogenesis has been connected to the EMT-triggered tumor initiation from cancer stemness [36]. The expression of VEGFA in bladder cancer specimens was substantially increased compared to those of normal mucosa (KOPPARAPU et al., 2013) and is regarded as a predictively prognostic biomarker in bladder cancer [37]. Patients who have higher *VEGFA* mRNA-expressing tumors usually showed an unfavorable survival [38]. Given this situation, the prominent role of VEGFA for tumor vasculature has been recognized as a feasible target for anticancer treatment. To date, various anti-VEGF–VEGFR agents such as anti-VEGFA neutralizing monoclonal antibodies (e.g., Bevacizumab, Aflibercept), anti-VEGFR antibodies (e.g., Ramucirumab), VEGFR tyrosine kinase inhibitors (e.g., Vandetanib) and small-molecule inhibitors of tyrosine kinase inhibitors (e.g., Sunitinib, Sorafenib, Pazopanib) have undergone clinical trials for solid tumor [39]. Combined first-/second-line chemotherapy with bevacizumab substantially raised the overall survival (OS) and progression-free survival (PFS) in patients with metastatic colorectal cancer (mCRC) and advanced cervical cancer [40,41] under a two-arm randomized phase III trial. However, adding ramucirumab to docetaxel in platinum-refractory UC represented favorable PFS yet had no significant effect on OS for RANGE trial [42]. Albeit a single-arm phase II trial for the combination of first-line

chemotherapy (gemcitabine and cisplatin, GC) with bevacizumab significantly prolonged UC patients' OS [43], the randomized phase III CALGB 90,601 (Alliance) study indicated that adding bevacizumab to GC treatment in UC patients had no strikingly effect on OS compared to those of the placebo group (GC treatment only) [44].

Our data suggested that the MVD, the consequence of tumoral angiogenesis, is significantly diverse in UC. Accordingly, a biomarker-based selection is mandatory to identify patients, which might be most beneficial via antiangiogenic therapeutics. Noticeably, antiangiogenic therapy has been reported to provoke hypoxia and inhibit nutrient supply. Consequently, neoplasm diverted its microenvironment toward hyperglycolysis to build a metabolic symbiosis: hypoxic tumor cells enforce the capacity of glycolysis, promoting the production of lactate and largely exported lactate via monocarboxylate transporter 4 (MCT4). Furthermore, tumor cells in the oxygen-sufficient regions utilize extracellular lactate to fuel the citric acid cycle for the accelerated oxidative phosphorylation. The metabolic symbiosis of hypoxic and normoxic tumor cells leads to the therapeutic resistance to antiangiogenic therapy. However, metabolic symbiosis collapses once the suppression of hyperglycolysis and lactate export [45]. Interestingly, our studies disclosed the CEBPD–has-miR429 signaling axis not only presented a proangiogenic property by regulating VEGFA but also promoted glycolysis through MYC-dependent and -independent signaling pathways. Moreover, we also demonstrated the expression of CEBPD could be remarkably upregulated by cisplatin in UC [15], which might partly explain the lack of survival advantage by the combination of gemcitabine, cisplatin and bevacizumab in the CALGB 90,601 (Alliance) trial. Taken together, a series of our studies suggested a more precise drug combination targeting angiogenesis could avoid activation of signaling cascades carrying resistance. Moreover, a biomarker-based design of antiangiogenic therapy and searching ways for CEBPD blockade for UC would be warranted.

Although there are current advantages of screening and remedy, the therapy still confronts many obstacles to overcome on account of the high heterogeneity of UC with the unfavorable outcome. In this study, we figured out the regulatory mechanism behind the VEGFA-induced neoangiogenesis through CEBPD-dependent hsa-miR-429 inhibition in UC. Accordingly, combining CEBPD with VEGFA as predictive strategies and therapy markers could tailor and enlarge the preventive and clinically prognostic management. This study could be beneficial to target the patients likely to apply for anti-VEGF targeted therapy in the future.

Supplementary Materials: The following supporting information can be downloaded at: <https://www.mdpi.com/article/10.3390/cells11040638/s1>, Table S1: VEGFA is a potentially predicted target for hsa-miR-429 by Miranda database (<http://cbio.mskcc.org/miRNA2003/miranda.html> (accessed on 16 January 2022)) described as our previous research paper [1].

Author Contributions: Conceptualization: T.-C.C. and C.-F.L.; methodology: T.-C.C., Y.-L.S. and C.-F.L.; investigation: T.-C.C., C.-H.H., Y.-L.S., S.K.H. and C.-F.L.; formal analysis: T.-C.C., K.-L.H., Y.-H.K. and C.-F.L.; resources: C.-H.H. and C.-F.L.; validation: C.-H.H., Y.-L.S. and S.K.H.; visualization: T.-C.C. and C.-F.L.; writing—original draft: T.-C.C.; writing—review and editing: C.-F.L.; funding acquisition: C.-F.L.; supervision: C.-F.L. All authors have read and agreed to the published version of the manuscript.

Funding: This work was supported by grants from the Ministry of Science and Technology of Taiwan (109-2628-B-384 -003, 109-2314-B-037-110 -MY3, and 110-2628-B-384-001-) and in part by grants from the National Health Research Institutes of Taiwan (CA-110-PP-11) and Chi Mei Medical Center.

Institutional Review Board Statement: This study and its use of UC tissues that were deidentified from the biobank were approved by the Ethics Committee and Institutional Review Board of Chi Mei Medical Center (IRB10207-001) and followed the ethical guidelines of the Helsinki Declaration and the regulations of our government.

Informed Consent Statement: As a rule, every participant signed informed consent before being enrolled into Biobank.

Data Availability Statement: Not applicable.

Acknowledgments: The authors thank Tzu-Ju Chen and Wan-Shan Li (Chi Mei Medical Center, Tainan, Taiwan) for assistance with pathological examination of tissue specimens. The authors also thank the BioBank of Chi Mei Medical Center.

Conflicts of Interest: The authors declare no conflict of interest.

References

- Clark, P.E.; Agarwal, N.; Biagioli, M.C.; Eisenberger, M.A.; Greenberg, R.E.; Herr, H.W.; Inman, B.A.; Kuban, D.A.; Kuzel, T.M.; Lele, S.M.; et al. Bladder cancer. *J. Natl. Compr. Canc. Netw.* **2013**, *11*, 446–475. [CrossRef]
- Taiwan Cancer Registry; Bureau of Health Promotion, Dept. of Health, Taiwan. The Incidence of Renal Pelvic and Ureteral Tumor in Taiwan. Available online: <https://cris.bhp.doh.gov.tw/pagepub/Home.aspx?itemNo=cr.q.10> (accessed on 11 December 2021).
- Chen, C.-H.; Dickman, K.; Moriya, M.; Zavadil, J.; Sidorenko, V.; Edwards, K.; Gnatenko, D.; Wu, L.; Turesky, R.; Wu, X.-R.; et al. Aristolochic acid-associated urothelial cancer in Taiwan. *Proc. Natl. Acad. Sci. USA* **2012**, *109*, 8241–8246. [CrossRef]
- Sung, H.; Ferlay, J.; Siegel, R.L.; Laversanne, M.; Soerjomataram, I.; Jemal, A.; Bray, F. Global Cancer Statistics 2020: GLOBOCAN Estimates of Incidence and Mortality Worldwide for 36 Cancers in 185 Countries. *CA Cancer J. Clin.* **2021**, *71*, 209–249. [CrossRef]
- Compérat, E.M.; Burger, M.; Gontero, P.; Mostafid, A.H.; Palou, J.; Rouprêt, M.; van Rhijn, B.W.G.; Shariat, S.F.; Sylvester, R.J.; Zigeuner, R.; et al. Grading of Urothelial Carcinoma and The New “World Health Organisation Classification of Tumours of the Urinary System and Male Genital Organs 2016”. *Eur. Urol. Focus* **2019**, *5*, 457–466. [CrossRef]
- Cancer Research UK. Bladder Cancer > Types, Stages and Grades. Available online: <https://www.cancerresearchuk.org/about-cancer/bladder-cancer/types-stages-grades> (accessed on 11 December 2021).
- Seront, E.; Machiels, J.P. Molecular biology and targeted therapies for urothelial carcinoma. *Cancer Treat Rev.* **2015**, *41*, 341–353. [CrossRef]
- Yassaie, O.; Chehroudi, C.; Black, P.C. Novel and emerging approaches in the management of non-muscle invasive urothelial carcinoma. *Adv. Med. Oncol.* **2021**, *13*, 17588359211039052. [CrossRef]
- National Collaborating Centre for Cancer (UK). *Bladder Cancer: Diagnosis and Management*; National Institute for Health and Care Excellence: London, UK, 2015.
- Chan, T.-C.; Chen, Y.-T.; Tan, K.T.; Wu, C.-L.; Wu, W.-J.; Li, W.-M.; Wang, J.-M.; Shiue, Y.-L.; Li, C.-F. Biological significance of MYC and CEBPD coamplification in urothelial carcinoma: Multilayered genomic, transcriptional and posttranscriptional positive feedback loops enhance oncogenic glycolysis. *Clin. Transl. Med.* **2021**, *11*, e674. [CrossRef]
- Balamurugan, K.; Sterneck, E. The Many Faces of C/EBP δ and their Relevance for Inflammation and Cancer. *Int. J. Biol. Sci.* **2013**, *9*, 917–933. [CrossRef]
- Ko, C.-Y.; Chang, W.-C.; Wang, J.-M. Biological roles of CCAAT/Enhancer-binding protein delta during inflammation. *J. Biomed. Sci.* **2015**, *22*, 6. [CrossRef]
- Sheshadri, N.; Sharan, S.; Sterneck, E. CEBPD is an early endoplasmic reticulum stress response gene implicated in breast cancer cell survival. *FASEB J.* **2017**, *31*. [CrossRef]
- Wang, S.-M.; Lin, W.-C.; Lin, H.-Y.; Chen, Y.-L.; Ko, C.-Y.; Wang, J.-M. CCAAT/Enhancer-binding protein delta mediates glioma stem-like cell enrichment and ATP-binding cassette transporter ABCA1 activation for temozolomide resistance in glioblastoma. *Cell Death Discov.* **2021**, *7*, 8. [CrossRef]
- Wang, W.J.; Li, C.F.; Chu, Y.Y.; Wang, Y.H.; Hour, T.C.; Yen, C.J.; Chang, W.C.; Wang, J.M. Inhibition of the EGFR/STAT3/CEBPD Axis Reverses Cisplatin Cross-resistance with Paclitaxel in the Urothelial Carcinoma of the Urinary Bladder. *Clin. Cancer Res.* **2017**, *23*, 503–513. [CrossRef]
- Wang, Z.; Zhu, Z.; Lin, Z.; Luo, Y.; Liang, Z.; Zhang, C.; Chen, J.; Peng, P. miR-429 suppresses cell proliferation, migration and invasion in nasopharyngeal carcinoma by downregulation of TLN1. *Cancer Cell Int.* **2019**, *19*, 115. [CrossRef]
- Chan, T.C.; Wu, W.J.; Li, W.M.; Shiao, M.S.; Shiue, Y.L.; Li, C.F. SLC14A1 prevents oncometabolite accumulation and recruits HDAC1 to transrepress oncometabolite genes in urothelial carcinoma. *Theranostics* **2020**, *10*, 11775–11793. [CrossRef]
- Li, C.F.; Tsai, H.H.; Ko, C.Y.; Pan, Y.C.; Yen, C.J.; Lai, H.Y.; Yuh, C.H.; Wu, W.C.; Wang, J.M. HMDB and 5-AzadC Combination Reverses Tumor Suppressor CCAAT/Enhancer-Binding Protein Delta to Strengthen the Death of Liver Cancer Cells. *Mol. Cancer* **2015**, *14*, 2623–2633. [CrossRef]
- Sanford, D.C.; DeWille, J.W. C/EBPdelta is a downstream mediator of IL-6 induced growth inhibition of prostate cancer cells. *Prostate* **2005**, *63*, 143–154. [CrossRef]
- Wang, D.; Cheng, X.; Li, Y.; Guo, M.; Zhao, W.; Qiu, J.; Zheng, Y.; Meng, M.; Ping, X.; Chen, X.; et al. C/EBP δ -Slug-Lox1 axis promotes metastasis of lung adenocarcinoma via oxLDL uptake. *Oncogene* **2020**, *39*, 833–848. [CrossRef]
- Balamurugan, K.; Mendoza-Villanueva, D.; Sharan, S.; Summers, G.H.; Dobrolecki, L.E.; Lewis, M.T.; Sterneck, E. C/EBP δ links IL-6 and HIF-1 signaling to promote breast cancer stem cell-associated phenotypes. *Oncogene* **2019**, *38*, 3765–3780. [CrossRef]
- Hartl, L.; Duitman, J.; Abernethy, H.L.; Chen, K.; Dijk, F.; Roelofs, J.; Dings, M.P.G.; Hooijer, G.K.J.; Hernandez, P.Y.; Pan, Q.; et al. CCAAT/Enhancer-Binding Protein Delta (C/EBP δ): A Previously Unrecognized Tumor Suppressor that Limits the Oncogenic Potential of Pancreatic Ductal Adenocarcinoma Cells. *Cancers* **2020**, *12*, 2546. [CrossRef]

23. Wang, Y.H.; Wu, W.J.; Wang, W.J.; Huang, H.Y.; Li, W.M.; Yeh, B.W.; Wu, T.F.; Shiue, Y.L.; Sheu, J.J.; Wang, J.M.; et al. CEBPD amplification and overexpression in urothelial carcinoma: A driver of tumor metastasis indicating adverse prognosis. *Oncotarget* **2015**, *6*, 31069–31084. [[CrossRef](#)]
24. Chuang, C.H.; Wang, W.J.; Li, C.F.; Ko, C.Y.; Chou, Y.H.; Chuu, C.P.; Cheng, T.L.; Wang, J.M. The combination of the prodrugs perforin-CEBPD and perforin-granzyme B efficiently enhances the activation of caspase signaling and kills prostate cancer. *Cell Death Dis.* **2014**, *5*, e1220. [[CrossRef](#)] [[PubMed](#)]
25. Chang, L.-H.; Huang, H.-S.; Wu, P.-T.; Jou, I.M.; Pan, M.-H.; Chang, W.-C.; Wang, D.D.H.; Wang, J.-M. Role of macrophage CCAAT/enhancer binding protein delta in the pathogenesis of rheumatoid arthritis in collagen-induced arthritic mice. *PLoS ONE* **2012**, *7*, e45378. [[CrossRef](#)] [[PubMed](#)]
26. Reddy, K.B. MicroRNA (miRNA) in cancer. *Cancer Cell Int.* **2015**, *15*, 38. [[CrossRef](#)] [[PubMed](#)]
27. Peng, Y.; Croce, C.M. The role of MicroRNAs in human cancer. *Signal Transduct. Target. Ther.* **2016**, *1*, 15004. [[CrossRef](#)] [[PubMed](#)]
28. Wu, C.L.; Ho, J.Y.; Hung, S.H.; Yu, D.S. miR-429 expression in bladder cancer and its correlation with tumor behavior and clinical outcome. *Kaohsiung J. Med. Sci.* **2018**, *34*, 335–340. [[CrossRef](#)]
29. Wu, C.-L.; Ho, J.-Y.; Chou, S.-C.; Yu, D.-S. MiR-429 reverses epithelial-mesenchymal transition by restoring E-cadherin expression in bladder cancer. *Oncotarget* **2016**, *7*, 26593–26603. [[CrossRef](#)]
30. Guo, C.; Zhao, D.; Zhang, Q.; Liu, S.; Sun, M.-Z. miR-429 suppresses tumor migration and invasion by targeting CRKL in hepatocellular carcinoma via inhibiting Raf/MEK/ERK pathway and epithelial-mesenchymal transition. *Sci. Rep.* **2018**, *8*, 2375. [[CrossRef](#)]
31. Qu, H.-C.; Huang, Y.; Mu, Z.-Y.; Lv, H.; Xie, Q.-P.; Wang, K.; Hu, B. Efficacy and Safety of Chemotherapy Regimens in Advanced or Metastatic Bladder and Urothelial Carcinomas: An Updated Network Meta-Analysis. *Front. Pharmacol.* **2020**, *10*. [[CrossRef](#)]
32. Chen, B.; Jin, H.; Wu, K. Potential role of vascular targeted therapy to combat against tumor. *Expert Opin. Drug Deliv.* **2009**, *6*, 719–726. [[CrossRef](#)]
33. Shibuya, M. Vascular Endothelial Growth Factor (VEGF) and Its Receptor (VEGFR) Signaling in Angiogenesis: A Crucial Target for Anti- and Pro-Angiogenic Therapies. *Genes Cancer* **2011**, *2*, 1097–1105. [[CrossRef](#)]
34. Shibuya, M. Vascular endothelial growth factor and its receptor system: Physiological functions in angiogenesis and pathological roles in various diseases. *J. Biochem.* **2012**, *153*, 13–19. [[CrossRef](#)] [[PubMed](#)]
35. Claesson-Welsh, L.; Welsh, M. VEGFA and tumour angiogenesis. *J. Int. Med.* **2013**, *273*, 114–127. [[CrossRef](#)] [[PubMed](#)]
36. Fantozzi, A.; Gruber, D.; Pisarsky, L.; Heck, C.; Kunita, A.; Yilmaz, M.; Meyer-Schaller, N.; Cornille, K.; Hopfer, U.; Bentires-alj, M.; et al. VEGF-Mediated Angiogenesis Links EMT-Induced Cancer Stemness to Tumor Initiation. *Cancer Res.* **2014**, *74*, 1566–1575. [[CrossRef](#)] [[PubMed](#)]
37. Huang, Y.J.; Qi, W.X.; He, A.N.; Sun, Y.J.; Shen, Z.; Yao, Y. Prognostic value of tissue vascular endothelial growth factor expression in bladder cancer: A meta-analysis. *Asian Pac. J. Cancer Prev.* **2013**, *14*, 645–649. [[CrossRef](#)] [[PubMed](#)]
38. Zaravinos, A.; Volanis, D.; Lambrou, G.I.; Delakas, D.; Spandidos, D.A. Role of the angiogenic components, VEGFA, FGF2, OPN and RHOC, in urothelial cell carcinoma of the urinary bladder. *Oncol. Rep.* **2012**, *28*, 1159–1166. [[CrossRef](#)]
39. Narayanan, S.; Srinivas, S. Incorporating VEGF-targeted therapy in advanced urothelial cancer. *Ther. Adv. Med. Oncol.* **2017**, *9*, 33–45. [[CrossRef](#)]
40. Hurwitz, H.I.; Tebbutt, N.C.; Kabbavar, F.; Giantonio, B.J.; Guan, Z.-Z.; Mitchell, L.; Waterkamp, D.; Taberner, J. Efficacy and safety of bevacizumab in metastatic colorectal cancer: Pooled analysis from seven randomized controlled trials. *Oncologist* **2013**, *18*, 1004–1012. [[CrossRef](#)]
41. Tewari, K.S.; Sill, M.W.; Penson, R.T.; Huang, H.; Ramondetta, L.M.; Landrum, L.M.; Oaknin, A.; Reid, T.J.; Leitao, M.M.; Michael, H.E.; et al. Bevacizumab for advanced cervical cancer: Final overall survival and adverse event analysis of a randomised, controlled, open-label, phase 3 trial (Gynecologic Oncology Group 240). *Lancet* **2017**, *390*, 1654–1663. [[CrossRef](#)]
42. Petrylak, D.P.; de Wit, R.; Chi, K.N.; Drakaki, A.; Sternberg, C.N.; Nishiyama, H.; Castellano, D.; Hussain, S.A.; Fléchon, A.; Bamias, A.; et al. Ramucirumab plus docetaxel versus placebo plus docetaxel in patients with locally advanced or metastatic urothelial carcinoma after platinum-based therapy (RANGE): Overall survival and updated results of a randomised, double-blind, phase 3 trial. *Lancet Oncol.* **2020**, *21*, 105–120. [[CrossRef](#)]
43. Hahn, N.M.; Stadler, W.M.; Zon, R.T.; Waterhouse, D.; Picus, J.; Nattam, S.; Johnson, C.S.; Perkins, S.M.; Waddell, M.J.; Sweeney, C.J. Phase II trial of cisplatin, gemcitabine, and bevacizumab as first-line therapy for metastatic urothelial carcinoma: Hoosier Oncology Group GU 04-75. *J. Clin. Oncol.* **2011**, *29*, 1525–1530. [[CrossRef](#)]
44. Rosenberg, J.E.; Ballman, K.A.; Halabi, S.; Atherton, P.J.; Mortazavi, A.; Sweeney, C.; Stadler, W.M.; Teply, B.A.; Picus, J.; Tagawa, S.T.; et al. Randomized Phase III Trial of Gemcitabine and Cisplatin With Bevacizumab or Placebo in Patients With Advanced Urothelial Carcinoma: Results of CALGB 90601 (Alliance). *J. Clin. Oncol.* **2021**, *39*, 2486–2496. [[CrossRef](#)] [[PubMed](#)]
45. Pisarsky, L.; Bill, R.; Fagiani, E.; Dimeloe, S.; Goosen, W.R.; Hagmann, J.; Hess, C.; Christofori, G. Targeting Metabolic Symbiosis to Overcome Resistance to Anti-angiogenic Therapy. *Cell Rep.* **2016**, *15*, 1161–1174. [[CrossRef](#)] [[PubMed](#)]